The Behaviour of Circular Footings on Silica Sand Subjected to Inclined Load

M S Poon
BE (Hons)
Research Student, Department of Civil Engineering, The University of Sydney, Australia
M J Cassidy
BE (Hons), DPhil, MIEAust
Lecturer, Centre for Offshore Foundation Systems, The University of Western Australia, Australia
D W Airey
MA, PhD
Senior Lecturer, Department of Civil Engineering, The University of Sydney, Australia
J P Carter
BE, PhD, DEng, FIEAust., CPEng.
Challis Professor, Department of Civil Engineering, The University of Sydney, Australia

Summary: The behaviour of circular shallow foundations on silica sand under inclined loads has been investigated by performing experimental model tests and numerical analyses. A series of displacement controlled loading tests was conducted on a small circular footing on sand with a range of relative densities, from loose to dense, and surcharge pressures from 0 to 50 kPa. The footing was loaded at four different angles from the vertical: 0", 10°, 20" and 30". Numerical analyses corresponding to the model tests were also performed using the strain hardening plasticity model, "Model C", developed at Oxford University for circular footings on dense Leighton-Buzzard sand. This paper will present some of the experimental results and show a comparison between the experimental results and the numerical predictions. It will be shown that Model C can make reasonable predictions of the inclined loading responses.

INTRODUCTION

Theoretical analyses to predict the bearing capacity of shallow foundations have advanced significantly since the well-known bearing capacity equation was proposed by Terzaghi (1943), based on a limit-equilibrium solution for the central vertical load case. Terzaghi's original equation was extended by a number of researchers (e.g., Vesic, 1973) to incorporate the influences of inclined and eccentric loadings. Although satisfactory estimations of bearing capacity can be achieved, the predictions depend on the product of an array of empirical coefficients, and this process results in only approximate rather than rigorous solutions.

Plasticity-based analyses to general bearing capacity problems were first suggested by Roscoe and Schofield (1957). This approach involves transforming the loading into three components: vertical, moment and horizontal. A yield surface is established within this (V, M, H) load space according to a given footing penetration. A number of experimental investigations conducted recently have shown that this approach is more powerful and consistent than the use of increasing numbers of empirical factors. Martin (1994) developed a complete plasticity model (Model B) based on a series of comprehensive tests of both shallow and deep circular footings on Kaolin clay. Houlsby and Cassidy (2002) developed a plasticity model (Model C) for drained loading of a circular foundation on dense (Leighton-Buzzard) sand based on experimental data by Gottardi & Houlsby (1995) and Gottardi *et al.* (1999). Cassidy *et al.* (2002) showed that, with some minor modifications, Model C could also reproduce the experimental data of Byrne and Houlsby (2001) for loose carbonate sand. The objective of this paper is to present and compare the observations from the experiments of circular footings on silica sand with various densities and surcharge pressures, with the predictions using Model C.

EXPERIMENTAL DETAILS

A series of inclined loading tests of circular footings on dense, medium and loose Sydney sand, under three different surcharge pressure (0 kPa, 25 kPa, 50 kPa). were conducted using a displacement controlled apparatus designed by Pan (1999) and modified by Poon (2003). The apparatus is schematically shown in Figure 1. It consists of a reaction frame, loading device, testing vessel, model footing, a system for generating surcharge pressures and equipment for measuring displacements, loads and surcharge pressure. The reaction frame comprises curved I-beams that can locate a servo-controlled hydraulic actuator at either 0"

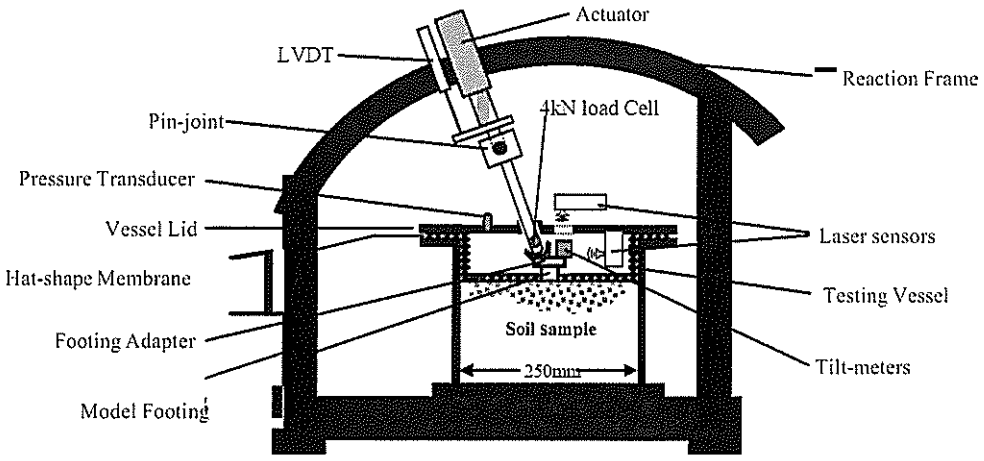

Figure 1. Apparatus for the Inclined Loading Tests

for vertical loading, or at inclinations to the vertical of 10°, 20°, and *30".* The testing vessel has an internal diameter of *250* mm and an internal depth of 300 mm. The metal footing has a milled smooth base and a diameter of *25* mm. The upper part of the footing assembly consists of an arrangement to locate the loading rod so that the line of action of the applied load remains at the centre of the footing base. The loading rod and the footing were not connected together, and hence different footing assemblies were required for different inclinations of load. The loading rod is connected to the loading ram by a pin-joint and has some freedom to rotate. The reasons for using this arrangement were to enable the footing to rotate and move freely in vertical and horizontal directions, and to avoid any kinematic restraint from the loading rod. It may be noted that the change in inclination of the rod during the test was minimal, as the footing movements were relatively small compared with the length of the rod. A hat-shaped latex membrane is sealed to the perimeter of the footing base in order to provide a barrier between the soil and the surcharge pressure. The surcharge pressure was achieved using air pressure delivered from a compressor and subsequently regulated through a manually adjusted valve.

The displacement of the loading rod was measured by a linear variable displacement transducer (LVDT) mounted adjacent to the actuator. The displacements of the footing, however, were measured independently by two laser displacement sensors and two tilt-meters. The two laser sensors measured the vertical and horizontal movement of the footing, while the two tilt-meters measured the rotation of the footing in the loading direction and any out-of-plane tilting. The traction load applied to the footing was measured by a 4 kN load cell mounted at the tip of the loading rod. The surcharge pressure applying on the sand was measured by a pressure transducer placed in the lid of the vessel. All transducer outputs were recorded by a high-speed data logger.

The soil used was *dry* Sydney sand (coefficient of uniformity = 2.05: D_{50} = 0.4 mm; G_s = 2.6; γ_{max} = *16.6* kN/m^3; γ_{min} = 14.3 kN/m^3). Samples were prepared at three relative densities using a sand raining technique: Dense (D_r = 100%), Medium (D_r = 50%) and Loose (D_r = *20%).* Details of the experiments and the sample preparation can be found in Poon *(2003).*

OUTLINE OF MODEL C

The model described here is known as Model C and is a strain hardening plasticity model for circular footings on dense sand. This model predicts the footing behaviour in terms of the force resultants acting on the footing and the corresponding footing displacement. Cassidy *et al (2002)* have also found the model to be applicable to loose carbonate sands with minor modifications. A detailed explanation of Model C is given in Cassidy (1999) and Houlsby and Cassidy *(2002).* However, some highlights of the model are presented here.

Yield Surface

Any penetration of the footing into the soil will establish a yield surface in (*V, M, H*) space, given by the following expression:

$$f(V,M/2R,H)=\left(\frac{H}{h_0V_0}\right)^2+\left(\frac{M/2R}{m_0V_0}\right)^2-\frac{2aHM/2R}{h_0m_0V_0^2} \qquad (1)$$

$$-\left(\frac{(\beta_1+\beta_2)^{(\beta_1+\beta_2)}}{\beta_1^{\beta_1}\beta_2^{\beta_2}}\right)^2\left(\frac{V}{V_0}\right)^{2\beta_1}\left(1-\frac{V}{V_0}\right)^{2\beta_2}=0$$

where V_0 is the bearing capacity under pure vertical load, R is the radius of the footing, and h_o, m_o, a, β_1, β_2 are dimensionless parameters. The recommended values of these parameters for silica sand were given in Cassidy *(1999)*and Houlsby and Cassidy *(2002)*and for loose carbonate sand in Cassidy *et al. (2002)*.

Elastic behaviour

Once the yield surface is established, any load paths within the surface will only result in elastic deformations. The elastic load-displacement relation is given as:

$$\begin{Bmatrix}\delta V\\ \delta M/2R\\ \delta H\end{Bmatrix}=2GR\begin{bmatrix}k_v & 0 & 0\\ 0 & k_m & k_c\\ 0 & k_c & k_h\end{bmatrix}\begin{Bmatrix}\delta w^e\\ 2R\delta\theta^e\\ \delta u^e\end{Bmatrix} \qquad (2)$$

where k_v, k_m, k_h, k_c are dimensionless constants. Typical values for these constants can be found in Ngo-Tran(*1996)*. The shear modulus G can be estimated by the formula:

$$\frac{G}{p_a}=g\sqrt{\frac{V}{Ap_a}} \qquad (3)$$

where p_a is the atmospheric pressure, V is the vertical load on the footing, $\mathbf{A}=\pi r^2$ is the plan area of the footing, and g is a dimensionless constant. A typical value of g is *230* for medium dense sand, however, this value depends on the relative density and reference can be made to Cassidy *et al. (2002)*.

Strain Hardening

While the shape of the yield surface is assumed constant, the size varies depending on a strain hardening law. For simplicity, the expansion of the yield surface is taken as a function of the vertical component of the applied load. For the modelling of dense silica sand, an empirical formula that models the peak profile and the post-peak softening of the vertical load-penetration curve was given by Houlsby and Cassidy *(2002)*as:

$$V_0=\frac{kw_p+\left(\frac{f_p}{1-f_p}\right)\left(\frac{w_p}{w_{pm}}\right)^2V_{0m}}{1+\left(\frac{kw_{pm}}{V_{0m}}-2\right)\left(\frac{w_p}{w_{pm}}\right)+\left(\frac{1}{1-f_p}\right)\left(\frac{w_p}{w_{pm}}\right)^2} \qquad (4)$$

where w_p is the plastic component of the vertical penetration, V_{0m} is the peak value of V_0, w_{pm} is the value of w_p at this peak. The parameters k and f_p represent hardening and softening behaviours respectively and can be varied to fit observed experimental data. For the modelling of loose carbonate sand, Cassidy *et al. (2002)* defined another empirical formula:

$$V_0=\frac{cw_p+k_2w_p^2}{k_1+w_p} \qquad (5)$$

where c, k_1 and k_2 are dimensionless parameters. Again the values of these parameters can be varied to fit observed data.

Plastic Potential

Using two association factors α_h, α_m, the plastic potential was defined by Cassidy *(1999)*as:

$$g(V,M/2R,H)=\left(\frac{H}{\alpha_h h_0 V_0'}\right)^2+\left(\frac{M/2R}{\alpha_m m_0 V_0'}\right)^2-\frac{2aHM/2R}{\alpha_h\alpha_m h_0 m_0 V_0'^2} \qquad (6)$$

$$-\left(\frac{(\beta_3+\beta_4)^{(\beta_3+\beta_4)}}{\beta_3^{\beta_3}\beta_4^{\beta_4}}\right)^2\left(\frac{V}{V_0'}\right)^{2\beta_3}\left(1-\frac{V}{V_0'}\right)^{2\beta_4}=0$$

It has been found that the experimental data can be fitted well if the association factors are taken as hyperbolic functions of the plastic displacement history, as proposed by Gottardi & Houlsby (1995). i.e.:

$$a_v=\frac{k'-\alpha_{hv}(u_p/w_p)}{k'+(u_p/w_p)} \tag{7}$$

$$\alpha_m=\frac{k'+\alpha_{mv}(2R\theta_p/w_p)}{k'+(2R\theta_p/w_p)} \tag{8}$$

For the modelling of dense silica sand, typical values were evaluated by Houlsby & Cassidy (2002) as: $\beta_3=0.55;\beta_4=0.65;\alpha_{hv}=2.5;$ $a_{rr}=2.15;$ $k'=0.125$. For the modelling of loose carbonate sand, Cassidy *et al.* (2002) recommended: $\beta_3=0.82;\beta_4=0.82;\alpha_{hv}=2.5;$ a_{rr} 3.0; $k'=2.6$.

MODELLING OF THE EXPERIMENTS

Numerical simulations using Model C were carried out for all the experiments involving a range of relative densities and surcharge pressures. For each surcharge pressure the differences between the experimental results and the numerical simulations showed similar trends with load inclination and relative density, but only comparisons of the results with 50 kPa surcharge pressure are presented here. The simulations were conducted by inputting the values of the measured footing displacements (v, θ, u) and calculating the corresponding loads (V, M, H).

Understanding of the experiment and choosing the right input data are essential for the modelling. Figure 2a shows the movement of the footing during an inclined loading test. While the loading rod is moving in a fixed direction (α° to the vertical), the footing is free to rotate about the tip of the rod and the centre of the footing base is displaced along a non-linear path (indicated by the dotted locus in Fig. 2a). This shows that the displacement of the footing is different from the loading trajectory. Therefore it is important that the displacements (v, 0, u) input into Model C are based on the path of the centre of the footing base and not the path of the loading rod.

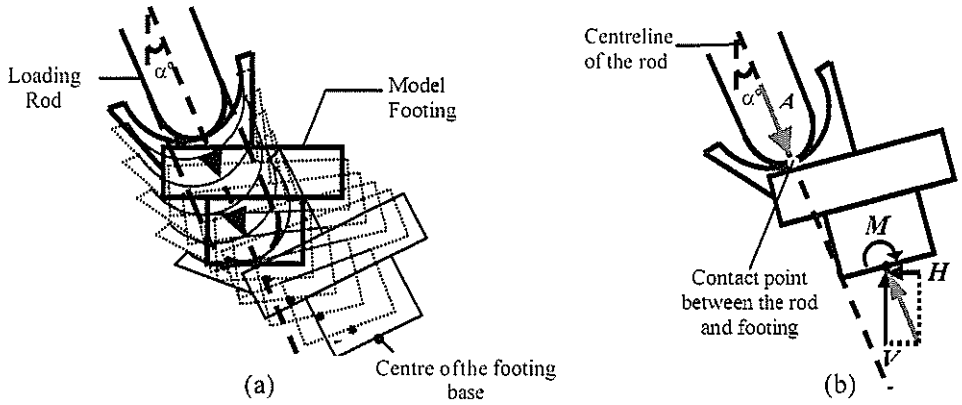

Figure 2. Movement of the Footing and Load Measurement

When the footing is rotating during a test, the rod also adjusts its position by rotating about the pin-joint until force equilibrium of the rod is achieved. If the surfaces in contact between the rod and footing are assumed frictionless, then equilibrium is achieved when the rod is acting on the footing in the axial direction (Poon, 2003). The vertical and horizontal components of force acting on the centre of the footing base are therefore $V=A\cos\alpha$ and $H=A\sin\alpha$, respectively (see Figure 2b), where A is the traction load measured in the rod and α is the angle of inclination of the rod. It is noted that the rotation of the rod during the test is minimal, any change in inclination of the rod is considered insignificant. The moment couple M of the footing is determined based on the moment of the resultant of V and H about the point of contact between the rod and footing. A detailed description on the derivation of M is given in Poon (2003).

Dense Sand

The results of the inclined loading tests on dense sand and the corresponding predictions using Model C are shown in Figure 3. Figure 3a shows the displacement paths of the rod for different inclinations. These paths

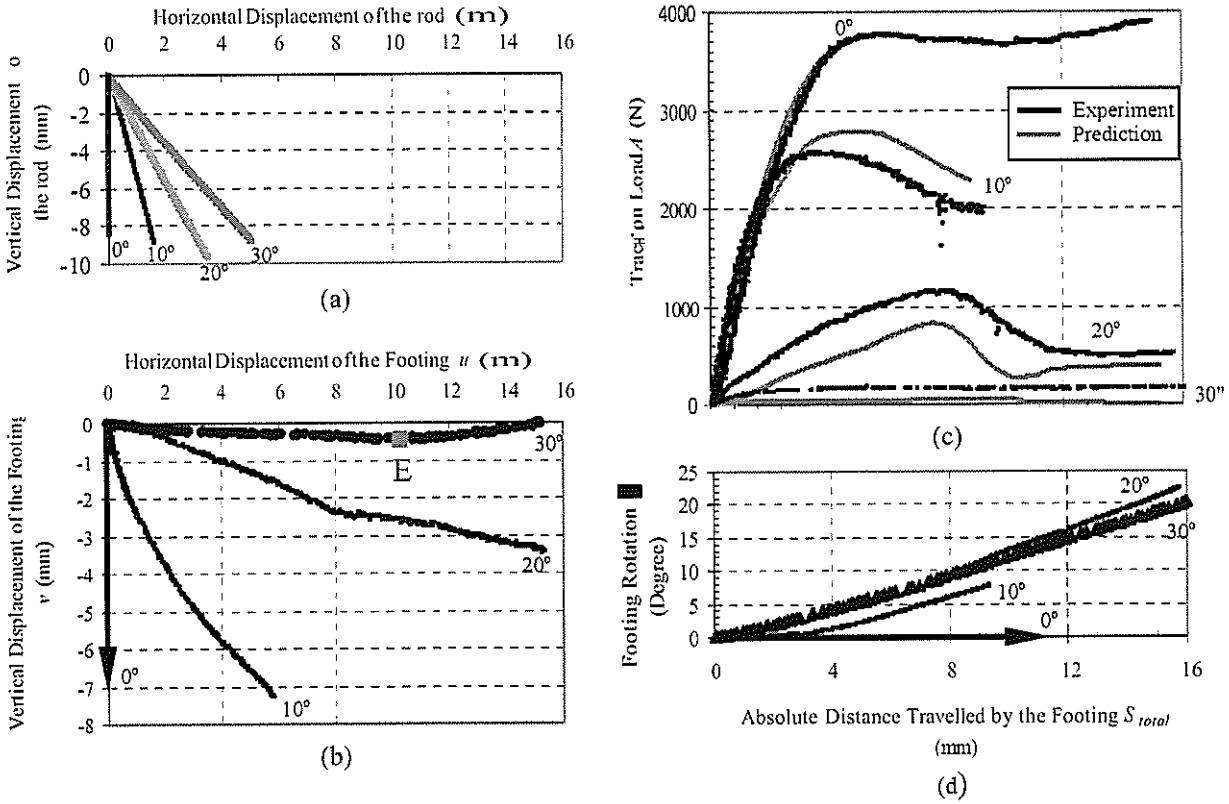

Figure 3. Results of Dense Sand and the Corresponding Predictions using Model C

are different from the corresponding deformation paths of the footing illustrated in Figure 3b. The deformation paths of the footing were reduced from the measurements of the tilt-meters and laser displacement sensors using a rigid body analysis. The displacement of the footing for the purely vertical test has not been monitored. However, as described in Poon (2003), the footing was seen visually being pushed downward and was therefore considered to have no tilting (as indicated by the horizontal arrow in Figure 3d) and no horizontal displacement (as indicated by the vertical arrow in Figure 3b). The out-of-plane rotations of the footing were small and have therefore not been shown in Figure 3. This confirms that the movement of the footing is confined to a three-degree of freedom problem with displacements (v, θ, u).

Figure 3c shows the measured and predicted traction load A, plotted against the absolute distance travelled by the footing $S_{total} = \sqrt{v^2 + u^2}$. By using the strain hardening equation of Byrne and Cassidy (2002) (Equation 4), and by taking the measured rod displacement from the purely vertical test (which is believed to be equal to the footing displacement for 0" loading), a theoretical curve that accurately represents the vertical test was constructed as shown in Figure 3c. Once the size of the yield surface was defined, the predictions of (V, H, M) of the footing for other loading inclinations were obtained by inputting into Model C the displacements (v, u, θ of different deformation paths and rotations of the footing.- Finally the traction load A predicted by Model C was simply calculated as: $A = \sqrt{V^2 + H^2}$.

As shown in Figure 3c. Model C over predicts the 10° loading but under predicts for 20° and 30° loadings. The simulations give good agreement in terms of the trends, particularly in terms of the point of maximum load and the post-peak softening. When the footing is loaded by a force applied at 30°, the footing has small vertical penetration because of the large component of sliding and rotation. In fact, the centre of the footing moves upwards after settling 0.4mm at instant E, as shown in Figure 3b. The reduction of the vertical penetration after this instant limits the expansion of the yield surface, and therefore the predicted load drops in contrast to the recorded load (Figure 3c), which remains constant.

The large components of horizontal displacement and rotation contribute to the under predictions for 20" and 30" loadings. This suggests that there is an inadequate contribution of radial hardening to the yield surface expansion. It is believed that if the strain hardening law were able to include the horizontal displacement and rotation as well as the vertical displacement, rather than being solely a function of the vertical deformation, as suggested by Byrne and Houlsby (2001), the predicted traction load would have been larger.

Loose Sand

For the modelling of loose silica sand, the yield shape, the plastic potential and the strain hardening equation were assumed to be the same as those used by Cassidy *et al.* (2002) in the modelling of loose carbonate sand. Figures 4a and b show the displacement paths and the rotations of the footing for different inclined loadings on loose sand. Figure 4c shows the observed and predicted traction loads. The prediction for 10° loading is exceptionally good. There is a slight under prediction for 20" loading and a substantial under prediction for 30" loading. Another set of simulations was carried out using a modified strain hardening equation that includes an expansion of the yield surface due to plastic rotation and horizontal displacements as well as vertical displacements. This was suggested by Byrne and Houlsby (2001) and was outlined in Cassidy *et al.* (2002). Again this gives an excellent prediction for 10" loading (indicated by the dotted curves in Figure 4c). The prediction for 20" loading is now higher, being much closer to the measured traction load. However, the prediction for 30" loading remains considerably lower than that measured. Overall, the simulations using this modified strain hardening equation give better predictions of the experimental data on loose silica sand.

Medium Dense Sand

For the modelling of medium silica sand, the strain hardening function (Equation 5) used to model the footing on loose sand has been used because the vertical load-penetration curves do not exhibit any peak profile. However, the yield surface shape and the flow rule are more difficult to choose due to less analogous experimental data. Figure 5a shows the results of simulations using the yield shape and flow rule of the loose sand. Model C gives a slight over prediction for 10° loading. However, when the input horizontal displacement and rotation are large as in 20°and 30° loading (see Poon, 2003), the simulations give substantial under predictions. Figure 5b shows the results of simulations using the yield shape and flow rule for dense sand. In contrast with the previous simulations, the 10° predicted load has been brought down slightly, being closer to the experimental curve. Moreover, the 20" and 30" predicted curves have risen markedly, giving better predictions of the recorded traction loads. Clearly, this suggests that better predictions of the experimental data on medium sand can be achieved using the dense sand yield shape and flow rule.

CONCLUSIONS

In this paper, comparisons have been made between Model C predictions and the experiments performed at the University of Sydney by Poon (2003). Owing to the nature of the experimental setup, the footings have

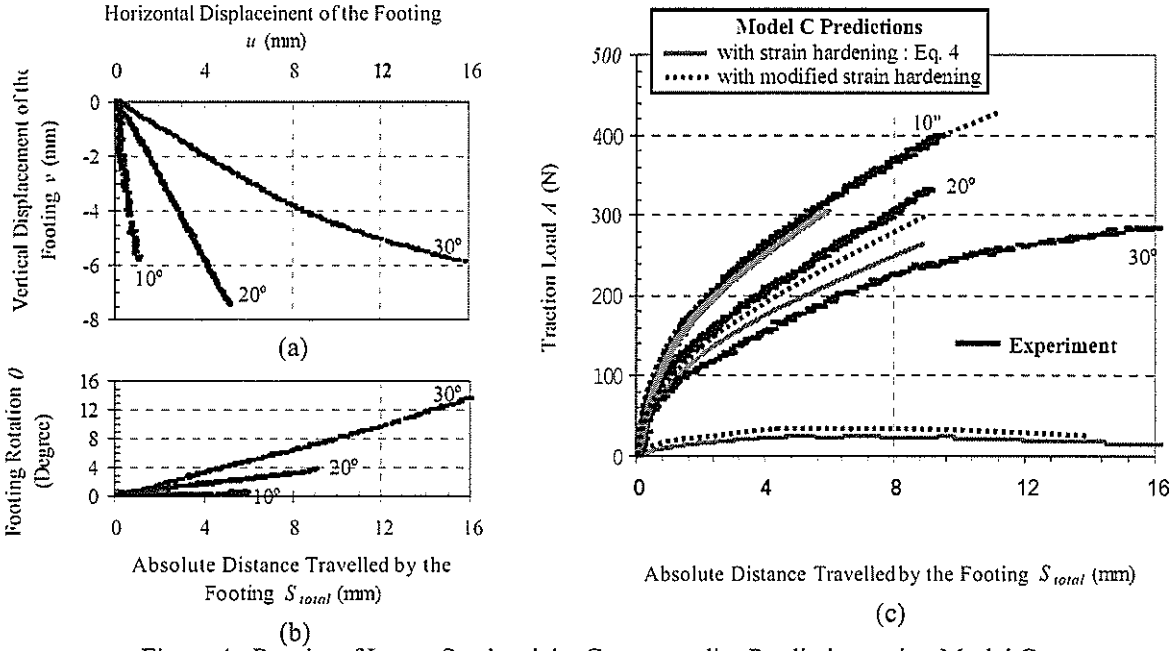

Figure 4. Results of Loose Sand and the Corresponding Predictions using Model C

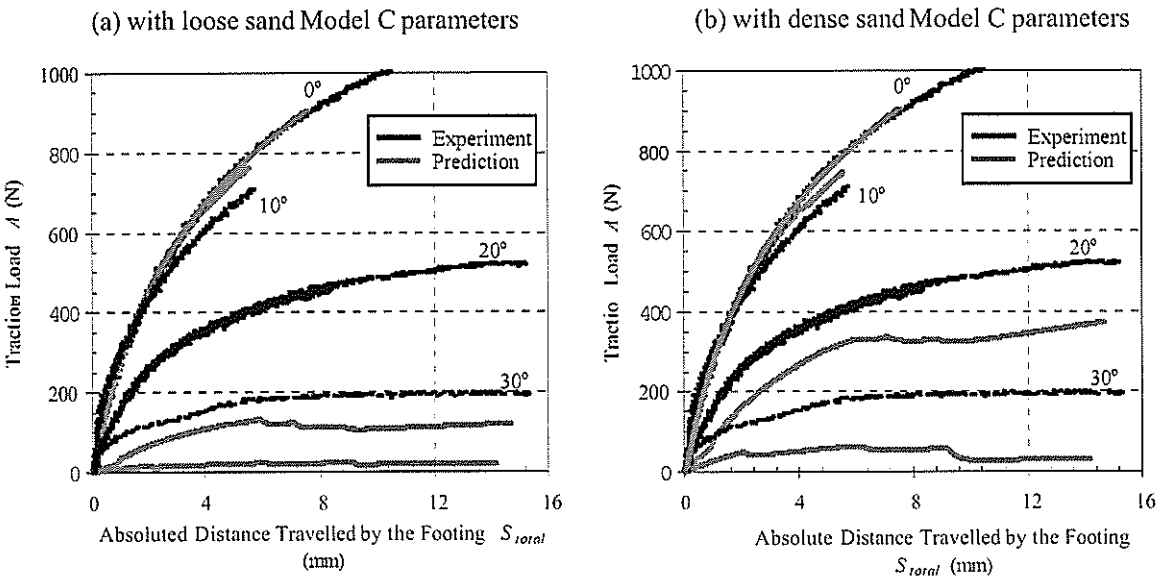

Figure 5. Observed and Predicted Traction Loads of Medium Dense Sand

been displaced along non-linear paths, rather than following the displacement of the loading rod at a fixed inclination. By choosing the same strain-hardening plasticity model as for dense Leighton-Buzzard sand, and with the displacements and rotation of the footing as the input data, the simulations for dense silica sand are successful in capturing the patterns of the recorded traction load. However, Model C gives under predictions when horizontal displacements and rotations are large. For the modelling of loose silica sand, the modified Model C as in Cassidy *et al.* (2002) is used. It is clear that better simulations can be achieved by using the strain hardening equation that includes the rotation, horizontal and vertical displacements, as suggested by Byrne and Houlsby (2001). However, substantial under prediction of the traction load resulted when there were large components of horizontal displacement and rotation. For the modelling of medium dense sand, it has been shown that while using the non-peak profile strain hardening expression for the loose carbonate sand, Model C gives much more promising predictions by using the yield surface and the corresponding flow rule for the dense silica sand. In general, the comparisons show that Model C is performing well, although some refinements are needed. This paper gives further support for the approach of using plasticity-based models (such as Model C) for shallow foundation problems.

REFERENCES

Byrne, B.W. and Houlsby, G.T. (2001). Observations of footing behaviour on loose carbonate sands, *Geotechnique* **51,** No. 5, 463-466.

Cassidy, M.J. (1999). *Non-linear analysis of jack-up structures subjected to random waves,* DPhil Thesis, The University of Oxford.

Cassidy, M.J., Byrne, B.W. and Houlsby, G.T. (2002). Modelling the behaviour of a circular footing under combined loading on loose carbonate sand. *Geotechnique* **52,** No. 10, 705-712.

Gottardi, G., Houlsby, G.T. and Butterfield, R. (1999). The plastic response of circular footings on sand under general planar loading. *Geotechnique* **49,** No. 4, 453-470.

Gottardi, G. and Houlsby, G.T. (1995). *Model tests of circular footings on sand subjected to combined loads,* OUEL Report No. 2071/95. Department of Engineering Science, The University of Oxford.

Houlsby, G.T. and Cassidy, M.J. (2002). A plasticity model for the behaviour of footings on sand under combined loading, *Geotechnique* **52,** No. 2, 117-129.

Martin, C.M. (1994). *Physical and numerical modelling of offshore foundations under combined loads.* DPhil Thesis, The University of Oxford.

Ngo-Tran, C.L. (1996). *The analysis of offshore foundations subjected to combined loading.* DPhil Thesis, The University of Oxford.

Pan, J. (1999). *The behaviour of shallow foundations on calcareous soil subjected to inclined loud.* PhD Thesis, The University of Sydney.

Poon, M.S.B. (2003). *The behaviour of shallow foundations on silica sand subjected to inclined loud.* PhD Thesis (in preparation)

Roscoe, K.H. & Schofield, A. N. (1956). The stability of short pier foundations in sand. *Br. Weld. J.,* August 343-354.

Terzaghi, K. (1943). *Theoretical Soil Mechanics,* John Wiley and Sons, New York.

Vesic, A.S. (1973). Analysis of Ultimate loads of shallow foundations. *J. Soil Mech. Found. Engng Div.,* ASCE 99, No. SM1, 45-73.